

Modelling transition phenomena of scientific coauthorship networks

Zheng Xie · Enming Dong · Dongyun Yi · Ouyang Zhenzheng · Jianping Li

Received: date / Accepted: date

Abstract In a range of scientific coauthorship networks, transitions emerge in degree distributions, correlations between degrees and local clustering coefficients, etc. The existence of those transitions could be regarded as a result of the diversity in collaboration behaviours of scientific fields. A growing geometric hypergraph built on a cluster of concentric circles is proposed to model two specific collaboration behaviours, namely the behaviour of leaders and that of other members in research teams. The model successfully predicts the transitions, as well as many common features of coauthorship networks. Particularly, it realizes a process of deriving the complex “scale-free” property from the simple “yes/no” experiments. Moreover, it gives a reasonable explanation for the emergence of transitions with the difference of collaboration behaviours between leaders and other members. The difference emerges in the evolution of research teams, which synthetically addresses several specific factors of generating collaborations, namely the communications between research teams, the academic impacts and homophily of authors.

Keywords Coauthorship network · Hypergraph · Geometric graph · Modelling

Z. Xie

College of Science, National University of Defense Technology, Changsha, 410073, China
E-mail: xiezheng81@nudt.edu.cn

E. Dong

College of Science, National University of Defense Technology, Changsha, 410073, China
E-mail: dongenming@gmail.com

D. Yi

College of Science, National University of Defense Technology, Changsha, 410073, China

Z. Ouyang

College of Science, National University of Defense Technology, Changsha, 410073, China

J. Li

College of Science, National University of Defense Technology, Changsha, 410073, China

1 Introduction

Coauthorship networks express collaborations graphically with nodes representing authors, and edges representing coauthor relationships. Since modern sciences increasingly involve collaborative research, the study of coauthorship networks has become an important topic of social science, especially of scientometrics [1]. It helps to understand the evolution and dynamics of scientific activities [2], measure the contributions of scientists [3], predict scientific success [4, 5], etc. The empirically observed coauthorship networks have some common local (degree assortativity, high clustering) and global (power-law degree distribution, short average distance) properties [6–9], according to which they are marked as scale-free and small-world networks. Some important models have been proposed to reproduce those properties, such as modeling the scale-free property by preferential attachment [10–16] or cumulative advantage [17], modeling the degree assortativity by connecting two non-connected nodes, which have similar degrees [18].

One explanation for the power-law tails of degree distributions is the inhomogeneous influences of nodes, which means that nodes with wider influences are likely to gain more connections. A specific example is that authors with large academic impacts, which often occupy a small fraction of the total authors in empirical coauthorship networks, capture voluminous collaborators. When using geometric graph theory (RGG) [19, 20] to analyze networks, such as citation networks, web-graphs, the impacts of nodes in scientific research or Internet can be modeled by attaching specific geometric zones to nodes [21–23]. Likewise our previous geometric graph model for coauthorship networks [24], which is built on a circle and reproduces the aforementioned features of coauthorship networks at certain levels.

Besides the academic impacts, the homophily of authors in the sense of geographical distances and research interests is another factor of generating collaborations [25, 26]. Comparing with topological graph models, an advantage of our model in Ref [24] is that it models the homophily by spatial coordinates of nodes. However, this model generates all authors at one time, so it cannot express the formation process of coauthorship networks. A growing geometric hypergraph is proposed here to model this process. It is built on a cluster of concentric circles, where each circle has a time coordinate.

Different from our previous model, the new model imitates the collaborations in and between research teams in dynamic ways. The main collaborations occur in the same research team, the mechanism of which synthetically expresses the influences of the homophily and the academic impacts of authors on collaborations in geometrical ways. Our analysis demonstrates that the model can also capture the aforementioned features of the empirical data.

Interesting phenomena of the empirical data are the transitions emerged in degree distributions $P(k)$, average local clustering coefficient and average degree of neighbors as functions of degrees ($C(k)$, $N(k)$). The data features are different in the two regions of k splitted by cross-over regions or tipping points. For example, the $P(k)$ of each empirical data emerges a generalized Poisson

and a power-law in small and large k regions respectively, where there exists a cross-over between the two regions. Our model successfully reproduces the shapes of those functions (much better than our previous model [24]) as well as their transitions, and gives reasonable explanations for those transitions.

The components of authors with voluminous collaborators are analyzed. The members of large “article team”s [17] are large degree authors. Each of such team is a group of researchers appeared as authors in an article. It is found that when removing large article teams, the degree distributions still have a power-law tail. Our model provides a reasonable explanation for the finding: the power-law tails are caused by the articles with many authors as well as the leaders of large research teams.

This report is organized as follows: the model and data are described in Sections 2 and 3 respectively; the degree distribution, clustering and assortativity are analyzed in Sections 4 and 5 respectively; the conclusion is drawn in Section 6.

2 The model

In reality, most researchers belong to research teams in universities and research institutes. For each research team, one or several researchers are responsible for the running of the team as leaders. “Research teams” and their “leaders” are the main objects in our model, which have been used in Ref [24]. The term “article team” in Ref [17] is also adopted by the model.

Our model creates “authors” (nodes) by a unit intensity Poisson process on a cluster of concentric circles, and randomly selects some nodes as “leaders” to attach specific geometric zones imitating their academic impacts. For each leader, a research team is formed by the nodes within the influential zone of the leader (Fig 1). Unlike the “lead authors” who are in charge of “article teams” in S. Milojević’s model [17], the leaders in our model are in charge of research teams, and concurrently play the roles of lead authors in article teams.

Inspired by the processes of generating coauthorship networks, the model generates hypergraphs first (in which authors are regarded as nodes and article teams as hyperedges), then extracts simple graphs from the hypergraphs (in which edges are formed between every two nodes in each hyperedge). Note that the isolated nodes are ignored, and the multiple edges are treated as one.

Since new articles are published per week or month, coauthorship networks evolve over time. Our model aims at simulating the evolution processes, especially the self-organizing formation of research teams in the processes. For this purpose, the numbers of hyperedges and nodes in the model are growing over time t . Parameter t can be explained as the t -th unit of time, such as t -th week, t -th month, etc.

The distribution of hyperedge sizes is an input of our model (an output of S. Milojević’s model [17]). The empirical distributions of hyperedge sizes appear a hook head and a fat tail, which can be sufficiently fitted by generalized

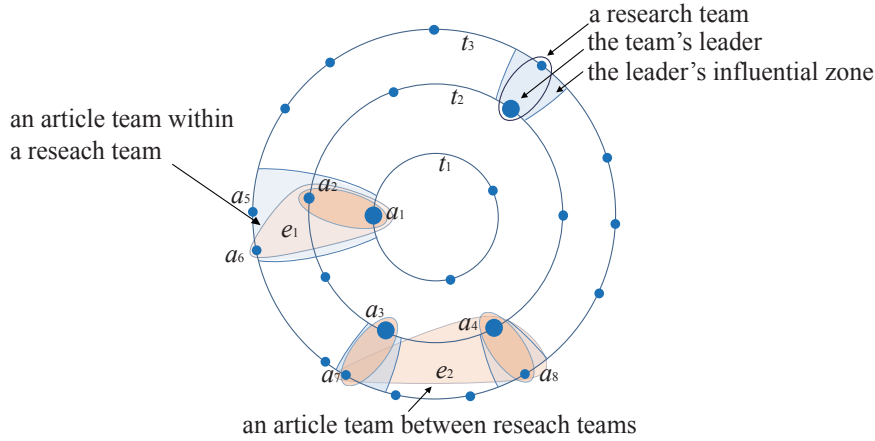


Fig. 1 Illustration of the model. The leaders (large nodes) have zones representing their academic impacts, the sizes of which change over time. The set of nodes in a zone (blue area) is regarded as a research team, and the set of nodes in a hyperedge (red area) as an article team. The sizes of research teams are in proportion to geometric sizes.

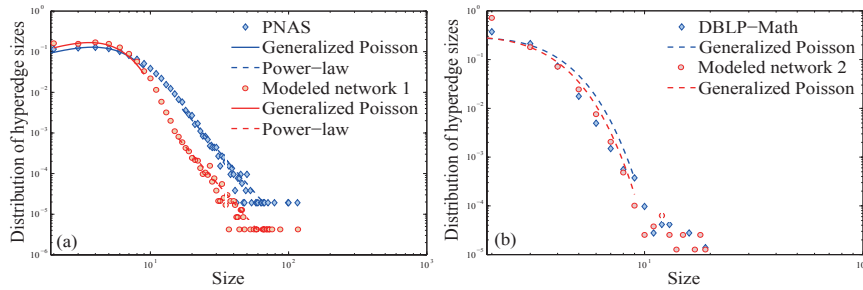


Fig. 2 The distributions of hyperedge sizes. Panels show the distributions of two modeled hypergraphs (parameters of which are listed in Section 3), PNAS 1999-2013 and DBLP-Math 1956-2013 respectively. The root mean squared errors (RMSE, used for measuring the goodness of fit) are 0.015 (generalized Poisson), 0.002 (power-law) for PNAS. 0.015 (generalized Poisson), 0.002 (power-law) for Modeled network 1, 0.113 for DBLP-Math, and 0.113 for Modeled network 2.

Poisson and power-law distributions respectively (Fig 2). For such kind of distributions, we denote their probability density function (PDF) by $f(x)$, $x \in \mathbb{Z}^+$. Denote the PDFs of generalized Poisson and power-law by $f_1(x) = a(a + bx)^{x-1}e^{-a-bx}/x!$ and $f_2(x) = cx^{-d}$ respectively, where $a, b, c, d \in \mathbb{R}^+$, and x belongs to some subsets of \mathbb{Z}^+ . We can generate random variables of an $f(x)$ with head $f_1(x)$ and tail $f_2(x)$ by sampling random variables of $f_1(x)$ and $f_2(x)$ with probability q and $1 - q$ respectively.

Based on the above assumptions, build a hypergraph on a cluster of concentric circles S_t^1 , $t = 1, \dots, T$ as follows:

1. Coordinate and influential zone (simply ‘zone’ hereafter) assignment
For time $t = 1, 2, \dots, T$ do:

Sprinkle N_1 nodes as potential authors uniformly and randomly on a circle S_t^1 . Identify each node, e.g. i , by its spatio-temporal coordinates (θ_i, t_i) , where t_i is the generating time of i ;

Select N_2 nodes from the new nodes randomly as leaders to attach specific zones: the zone of a leader, e.g. j , is defined as an interval of angular coordinate with center θ_j and length $\alpha(\theta_j)t_j^{-\beta}t^{\beta-1}$, where $\alpha(\theta_j)$ is a piecewise constant non-negative function of $\theta_j \in [0, 2\pi)$, and $\beta \in [0.5, 1]$;

2. Connection rules (simply ‘Rule’ hereafter)

For time $t = 1, 2, \dots, T$ do:

(a) For each new node i , search the existing leaders whose zones cover i . For each such leader j , generate a hyperedge with size m by grouping together i , j and $m - 2$ neighbors of j nearest to i , where m is a random variable drawn from a given $f(x)$ or the number of j ’s neighbors plus two if the former is larger than the latter.

(b) Select N_3 existing nodes (no distinction is made between leaders and non-leaders) with non-zero degree randomly. For each selected node l , generate a hyperedge by grouping together l and $m - 1$ randomly selected nodes with the same degree of l , where m is a random variable drawn from a given $f(x)$ or the number of nodes with the same degree of l if the former is larger than the latter.

Here randomly selecting means sampling without replacement. In reality, most article teams are subsets of some research teams, which are often formed by a leader and some members of the leader’s research team who have similar research interests. This collaboration mode is imitated by Rule (a), which groups together a certain number of nearest nodes and their leader as a hyperedge. Meanwhile, a few article teams are unions of some subsets from different research teams, even from different countries [27]. Such teams are very likely to appear in interdisciplinary articles, which account a relatively small fraction of total research articles. For example, the proportion of the articles marked as interdisciplinary ones in PNAS 1999-2013 is 5.7% [28]. The collaborations between research teams are modeled by Rule (b), which gives a possibility to connect the nodes in different research teams. Researchers can join different research teams. This phenomenon is equivalently imitated by Rule (b) to some extents. In this rule, grouping together certain numbers of nodes with the same degree is the simplest expression of the degree assortativity of authors in empirical data: authors prefer to collaborate with other authors with similar degrees [25]. More reasonable expressions of degree assortativity still need further research.

The way of generating hyperedges is different from that of our previous model [24], i.e. a new node will coauthor with its leaders, and some existing members of its leaders’ research team, which are nearest to it in the sense of space. Therefore, in the end, the authors (who could be non-leaders) with high scientific ages can write articles together with the authors who are not their nearest neighbors, since the nearest neighbors may not be generated when the articles were written. This difference causes the diversity of scientific ages not

only for leaders (which is addressed by the model in Ref [24]), but also for non-leaders. As shown in Fig 1, when the new author a_6 at time t_3 writes an article (which has three authors), it should coauthor with its leader a_1 and one nearest existing nodes in the research team of a_1 , namely a_2 , but not the nearest one a_5 .

The parameters of the model can be estimated from empirical data. For example, the collaborator numbers of authors (the degrees of nodes) in the empirical data are not very large. It means the value of $\alpha(\cdot)$ should be small, when N_1 is large. In reality, the leaders occupy a small fraction of the total researchers (potential authors), so N_2 is supposed to be far less than N_1 . Meanwhile, the number of article teams within a research team is far more than that between research teams, so N_3 is supposed to be small. In practice, N_3 could be a decimal belonging to the interval $[0, 1]$, which means implementing Rule (b) under probability N_3 at each time step.

The sizes of leaders' academic impacts and research teams are imitated by the sizes of zones. For a leader i , the size of its research team (the number of members in its research team) is $\delta\alpha(\theta_i)t_i^{-\beta}t^{\beta-1}$ at time $t > t_i$, where $\delta = N_1/(2\pi)$. Hence the cumulative size of the research team is

$$n(\theta_i, t_i, t) = \delta \times \left(\sum_{s=t_i+1}^t \alpha(\theta_i)t_i^{-\beta}s^{\beta-1} \right) \approx \frac{\alpha(\theta_i)\delta}{\beta} \left(\frac{t}{t_i} \right)^\beta. \quad (1)$$

There are some intuitive explanations for the formula (1). Firstly, the value of $t - t_i + 1$ is interpreted as the scientific age of a researcher, namely a researcher spending more time on research would have a larger academic impact and more collaborators as well. Hence it is reasonable to consider the sizes and cumulative sizes of research teams as increasing functions of scientific age, consequently decreasing functions of t_i . Secondly, the cumulative sizes of research teams will increase over t due to the continuously coming collaborators (e.g. tutors may have new students every year). Thirdly, the research team sizes may be different in research fields, so $\alpha(\cdot)$ is introduced to the formula. In addition, academic impacts of a leader, so the increment of cumulative research-team size could be considered to shrink over time ($\partial^2 n(\theta_i, t_i, t)/\partial t^2 < 0$) due to the process of retirements or activity decreases. Unlike articles, the aging of authors appears only for the data with large time span. The authors in PNAS 1999-2013 have no aging phenomenon on average, which will be discussed elsewhere. Hence the major role of the factor $t^{\beta-1}$ in the formula of zonal sizes is to tune the exponent of power-law.

3 The data

In order to test the universal reproduction ability of the proposed model, we analyze two empirical coauthorship networks from two metadata with different collaboration levels (Tab 1). One is DBLP-Math, which is constructed from 72,269 articles published in 54 mathematical journals during 1956–2013.

The article data are obtained from the database DBLP on <http://dblp.uni-trier.de/xml/dblp>. The other one is PNAS, which is constructed from 52,803 articles published in the Proceedings of the National Academy of Sciences (PNAS, <http://www.pnas.org>) during 1999–2013.

In order to analyze the components of authors with large degrees, Sub-PNAS, a sub-network of PNAS, is extracted from the articles, the numbers of authors in which are less than the boundary point of the generalized Poisson part in the distribution of hyperedge sizes. The point is detected by the algorithm in Tab 2. The inputs are hyperedge sizes, $g(\cdot) = \log(\cdot)$ and $h(\cdot) = f_1(\cdot)$.

In the process of extracting networks from those metadata, authors are identified by their names appeared in their articles. It is a reliable way to distinguish authors from one another in most cases. However, it will mistake one author as two if the author changes his/her name in different articles, and two authors as one if they have the same name. Those deficiencies will cause the inaccurate for the empirical networks to express real coauthorships. Fortunately, the considered statistical properties of those networks show similarities to those of the coauthorship networks with specific operations of author name disambiguation [7, 8]. So using those networks is rational at certain levels.

Two synthetic coauthorship networks are generated to reproduce several properties of the empirical data respectively. In detail, for Modeled network 1 (2), $q = 0.9625$ (0.999) in Rule (a), $q = 1$ (0.999) in Rule (b), $f_1(x)$ is the Poisson distribution with mean 5.5 (2.3), and $f_2(x) \propto x^{-3.7}$, $x \in [10, 150]$ ([11, 20]) in Rules (a-b). Set $T = 4,500$ (9,000) and $N_1 = 100$ (15) to make the number of nodes comparable to that of the empirical data in magnitude. Set $N_2 = N_1/5$, $\alpha = 0.19$ (0.2) and $\beta = 0.42$ (0.43) to make the average degree comparable to that of the empirical data. Set $N_3 = 1$ (0.5) to make the generated network have a giant component and the node proportion of the giant component comparable to that of the empirical data.

In order to make the synthetic networks capture a range of empirical features at certain levels, e.g. degree distributions, we have attempted many times to find above parameters. Since the model is stochastic, we generate 20 networks with the same parameters, and compare their statistical indicators in Tab 1. The finding is that the model is robust on those indicators.

One shortcoming of our model is that in order to make some common features of modelled networks fit those of the empirical data, Modeled network 1's distribution of hyperedge sizes does not fit that of PNAS very well, only captures the features of hook-head and fat-tail.

The indicator MO in Tab 1 shows that the same as the empirical networks, the modeled networks have clear communities. The reason is that the nodes in the same research team probably belong to the same community due to Rule (a), and the connections between research teams are small due to Rule (b). Thus edges within communities are significantly more than those between communities, which results to the clear community structures. The high GCC and small AP show the small-world property of the modeled networks. In addition, the distributions of component sizes are similar to those

Table 1 Specific statistical indicators of the analyzed networks.

Network	NN	NE	GCC	AC	AP	MO	PG	NG
PNAS	201,748	1,225,176	0.881	0.230	5.736	0.884	0.868	4,848
DBLP-Math	68,183	99,116	0.756	0.157	9.256	0.935	0.477	15,492
Modeled network 1	193,655	1,261,131	0.788	0.228	5.957	0.952	0.817	6,230
Modeled network 2	70,921	121,685	0.687	0.095	9.429	0.946	0.606	8,940
Sub-PNAS	200,170	1,158,503	0.881	0.097	5.806	0.882	0.867	4,869

The indicators are the numbers of nodes (NN) and edges (NE), global clustering coefficient (GCC), assortativity coefficient (AC), average shortest path length (AP), modularity (MO, calculated by the Louvain method [29]), the node proportion of the giant component (PG), and the number of components (NG). The values of AP of the first, third and fifth networks are calculated by sampling 15,000 pairs of nodes.

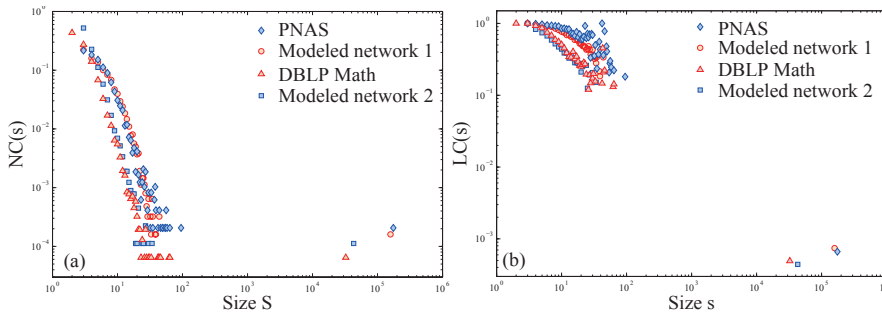


Fig. 3 The distributions of component sizes $NC(s)$ and the average proportion of the largest cliques in s -components (components with size s) $LC(s)$ of the first four networks in Tab 1. If there is an s that makes $LC(s) \approx 1$, it means the s -components are nearly fully connected.

of the empirical data respectively (Fig 3), the reason of which is the same as our previous model in Ref [24], so is omitted here.

4 The components and transitions of degree distributions

The degree distributions of coauthorship networks (the distributions of collaborators per author) appear two common features, namely a hook head and a fat tail, which can be sufficiently fitted by generalized Poisson and power-law distributions respectively. In statistics, if regarding authors of a coauthorship network as samples, such a mixture distribution means those samples come from different populations, namely the collaboration mode of authors with small degrees differs from that with large degrees. In reality, the main fraction of the authors are teachers and students in institutes and universities, who can be regarded as two different populations. The collaboration modes of students and teachers are different. Many students only write a few articles, and do not write after graduations, but their teachers could continuously write articles collaborating with their new students or other researchers.

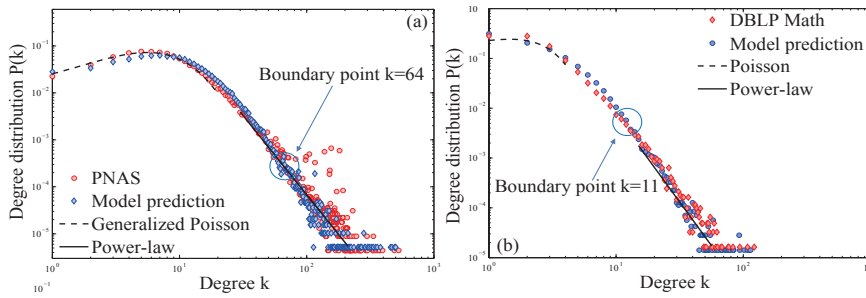


Fig. 4 The degree distributions of the first four networks in Tab 1. The fitting functions are the PDFs of generalized Poisson and power-law for the heads and tails respectively. The RMSEs are 0.01 (generalized Poisson), 0.019 (power-law) for PNAS and 0.009 (Poisson), 0.02 (power-law) for DBLP-Math. The fittings pass the KS test at significance level 5%.

The analytical (Appendix) and numerical evidences (Fig 4) illustrate the ability of our model in reproducing the empirical degree distributions. The tunable parameters of the formula for the sizes of influential zones give our model flexibility for empirical networks in diverse fields. Specifically, the power exponents of fat tails and the hook peaks can be tuned by β and the expected value of f_1 respectively. Here we give an intuitionistic explanation to show how the geometric aspect of the model is actually necessary to fit the empirical degree distributions.

There are two essential questions for the emergence of such degree distributions: Why the distributions emerge Poisson and power-law; Is there any essential relation between them? We attempt to give an answer by analyzing and simulating collaboration modes. The event that whether a researcher joins a research team can be treated as a “yes/no” experiment. So the size of a research team is equal to the number of successes in a sequence of n experiments, where n is the number of candidates for the members of the research team. Approximate the probability p of “yes” by its expected value \hat{p} , and suppose those “yes/no” experiments to be independent. Then, the sizes of research teams will follow a binomial distribution $B(n, \hat{p})$. When n is large and \hat{p} is small, $B(n, \hat{p})$ can be approximated by a Poisson distribution with mean $n\hat{p}$ (Poisson limit theorem). The value of $n\hat{p}$ is not a constant due to the diversity of research teams’ attractive abilities.

Our model generates a range of Poisson distributions. Nodes are generated according to a Poisson point process, hence the number of nodes covered by a zone is a random variable drawn from a Poisson distribution with an expected value in proportion to the zonal size. The diversity of expected values is expressed by the various sizes of leaders’ influential zones.

In reality, the “yes/no” experiments could be affected by previous occurrences, e.g. students sometimes introduce their research teams to their juniors. So for small research teams, it is reasonable to regard their sizes as random variables drawn from a range of generalized Poisson distributions (which allow the probability of an event’s occurrence to affect by previous events [30]). For

large research teams, the numbers of their candidates are large enough that the “yes/no” experiments can be regarded to be independent. So their sizes could be regarded as random variables drawn from a range of Poisson distributions with sufficiently large means.

Now we analyze the reason for the emergence of Poisson and how it is captured by the model. The authors with small degrees usually belong to only one small article team, or come from small research teams, the sizes of which are no larger than the mean sizes of article teams. For the first case, the empirical data show that the heads of the distributions of hyperedge sizes are well fitted by generalized Poisson distributions (Fig 2). Hence the degrees of authors who belong to only one small article team are equal to the size of the article team minus one, hence also follow generalized Poisson distributions. For the second case, authors in those small research teams probably write articles together. Ignoring the minority of collaborations between research teams, the degrees of those authors are close to the sizes of corresponding research teams minus one, therefore also follow generalized Poisson distributions. The good data-model fit of the Poisson part is due to that the two cases are addressed by the input of hyperedge sizes and the influential zones with small sizes respectively.

Next we turn to the power-law. The authors with large degrees are the authors of large article teams or the leaders of large research teams. For the first case, the empirical data PNAS shows that the sizes of large article teams follow a power-law distribution with exponent $\gamma = -3.96$ (Fig 2). If supposing each author belongs to only one of such article teams, then the degrees of those authors are drawn from a power-law distribution with exponent $\gamma - 1$. However, the supposition is not fully established in reality (Fig 5b). For the second case, the leaders usually collaborate with all of their team members. Ignoring the minority of collaborations between research teams, the degree of a such leader is close to the size of his/her research team minus one. A power-law appears when averaging a range of Poisson distributions, the expected values of which are relatively large and satisfy the power-law functional relation ($\propto s^{-\beta}$) preseted in the model.

The mathematical deduction of generating power-law from Poisson is proposed in Appendix, where the calculations in Eq 4 are inspired by some of the same general ideas as explored in the cosmological networks [20]. In fact, the second case illustrates the relation between the Poisson and power-law. It shows that “scale-free”, namely the emergence of power-law tails, partly comes from many Poisson processes, consequently from many “yes/no” experiments. In this sense, coauthorship networks give good examples of “ $1+1 > 2$ ” for systems science and complexity.

At last we consider the boundary points of generalized Poisson parts in degree distributions. An algorithm is provided to detect those points by using some statistical technologies synthetically (Tab 2). Inputs are degrees as observations, $g(\cdot) = \log(\cdot)$ and $h(\cdot) = f_1(\cdot)$. Using $\log(\cdot)$ can rescale the differences between the fitting model and empirical data at different scales, which helps to detect the boundary points at small scales.

Table 2 Boundary point detection algorithm for PDFs.

Input: Observations $O_s, s = 1, \dots, n$, rescaling function $g(\cdot)$, fitting model $h(\cdot)$.
For k from 1 to $\max(O_1, \dots, O_n)$ do:
Fit $h(\cdot)$ to the PDF $h_0(\cdot)$ of $\{O_s, s = 1, \dots, n O_s \leq k\}$ by maximum-likelihood estimation;
Do Kolmogorov-Smirnov (KS) test for two data $g(h(t))$ and $g(h_0(t)), t = 1, \dots, k$ with the null hypothesis they coming from the same continuous distribution;
Break if the test rejects the null hypothesis at significance level 5%.
Output: The current k as the boundary point.

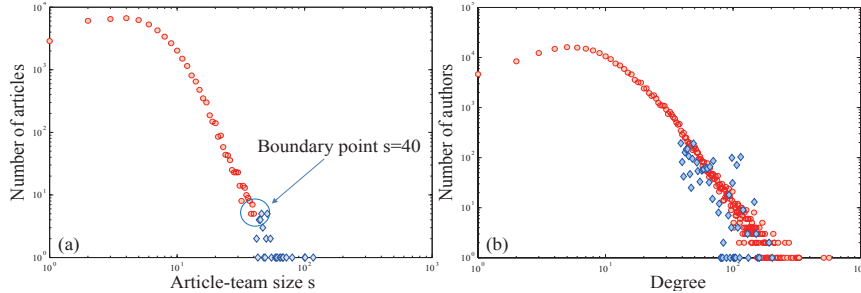


Fig. 5 The components of the authors with many collaborators. Panel (a) shows the distribution of article-team (hyperedge) sizes and its boundary point (the detecting way of which is described in Section 3) for PNAS 1999-2013. The red circles and blue diamonds in Panel (b) express the degree distributions of the networks extracted from the article teams with sizes $s < 40$ and $s \geq 40$ respectively.

The transition from Poisson to power-law is smooth in DBLP-Math, but nonsmooth in PNAS (Fig 4). A reason for the difference is that the components of large degree nodes in the two data are different. Authors with large degrees in PNAS partly come from large article teams (Fig 5), but DBLP-Math has no large article team. If an author only writes articles with small article teams, the growing process of his/her degree is smooth. In our model, this process is represented by the smoothly increasing process of each research team's cumulative size (Eq 1). Meanwhile, the model parameter q tunes the proportion of large article teams. Hence, when q is very small, the transitions of modeled networks, e.g. Modeled network 2, are smooth.

To further show the geometric aspect of the model is actually necessary in fitting the empirical degree distributions, we generate a random hypergraph with the same distribution of hyperedge sizes as that of Modelled network 2. The nodes of each hyperedge are selected randomly. The network has a community structure (MO= 0.434), small-world and degree-assortativity properties, but its degree distribution follows a generalized Poisson and has no power-law tail. Therefore, the power-law tails in the modeled distributions of collaborators per author have no direct relation with the corresponding distributions of hyperedge sizes.

5 Diversities in clustering behaviour and degree correlation

As global features, the positive Pearson correlation coefficient (PCC) of degrees between pairs of collaborated authors (degree assortativity) and high global clustering coefficient (GCC, the fraction of connected triples of nodes which also form “triangles”) are common in coauthorship networks. A general interpretation for degree assortativity of social networks is the homophily of nodes, namely similar people attract one another [25]. The homophily in research interests is the precondition of collaborations. The homophily is also an explanation for high GCC, because the relation of similarity between nodes is symmetric, reflexive and transitive.

It can be found that the clustering behaviour and degree correlation differ from the authors with small degrees to those with large degrees. Denote the average local clustering coefficient (LCC) and average neighbor degree of k -degree nodes by $C(k)$ and $N(k)$ respectively. Degree correlation can be measured by the slope of $N(k)$ [31]. If the function is increasing, nodes with large degrees connect to nodes with large degrees on average, which means the network is assortative.

There exist transitions in the $C(k)$ and $N(k)$ of the empirical data (Figs 6,7). The tipping points of those functions are detected by the algorithm in Tab 3. The inputs are $C(k)/N(k)$, $g(\cdot) = \log(\cdot)$ and $h(s) = a_1 e^{-((s-b_1)/c_1)^2} / h(s) = a_1 x^3 + a_2 x^2 + a_3 x + a_4$. Using the term “tipping point” is suitable for PNAS data, because the features in the two regions splitted by the points have significant difference. However, the term is not quite accurate for the $C(k)$ of DBLP-Math, because its transition is not so sharp. Using boundary point may be more suitable.

When k is larger than the tipping point, the $C(k)$ of each empirical data emerges a decreasing trend, which is proportional to $1/k$. Meanwhile, the PCCs of k and $N(k)$ in the two regions of k splitted by tipping points are $0.416/-0.025$ and $0.250/-0.046$ for PNAS and DBLP-Math respectively. The existence of tipping points in $C(k)$ and $N(k)$ provides an evidence for the difference between the collaboration behaviour of authors with small degrees and that with large degrees.

Table 3 Boundary point detection algorithm for general functions.

Input: Data vector $h_0(s)$, $s = 1, \dots, K$, rescaling function $g(\cdot)$, fitting model $h(\cdot)$
For k from 1 to K do:
Fit $h(\cdot)$ to $h_0(s)$, $s = 1, \dots, k$ by regression;
Do KS test for two data vectors $g(h(s))$ and $g(h_0(s))$, $s = 1, \dots, k$ with the null hypothesis they coming from the same continuous distribution;
Break if the test rejects the null hypothesis at significance level 5%.
Output: The current k as the boundary point.

The low LCCs and non-positive PCC of degree k and $N(k)$ in large k regions cannot be explained by homophily. We attempt to give an explanation in the following parts. The analysis in Section 4 has illustrated that authors in

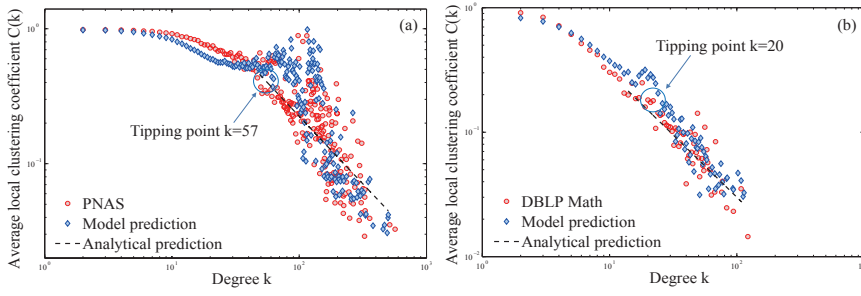


Fig. 6 The relation between local clustering coefficient and degree. The panels show the average local clustering coefficient of k -degree nodes for four networks in Tab 1 respectively. The RMSE for the theoretical prediction $C(k) \propto 1/k$ is 0.04597 for PNAS and 0.01476 for DBLP-Math.

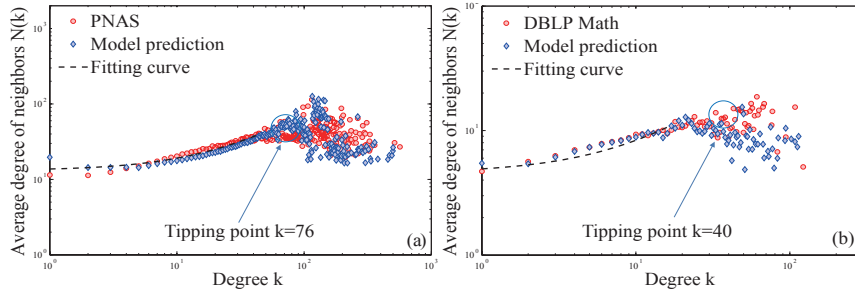


Fig. 7 The relation between degree and average degree of neighbors. The panels show k -degree nodes' average degree of their neighbors for four networks in Tab 1 respectively. The RMSE for the linearly increasing trend is 3.075 for PNAS and 1.313 for DBLP-Math.

small research teams (no larger than the mean size of article teams) are more likely to write articles together, and have small degrees on average. Hence the authors in a small research team may have high LCCs and similar degrees.

As the cumulative size of a research team increases over time, the degree difference emerges between the leader and non-leaders, because the leader usually collaborates with all members, but non-leaders only write a few articles with a few members on average. So the degrees of non-leaders, on average, do not increase with the growth of their leaders' degrees, which leads to the non-positive PCCs of k and $N(k)$ in large k regions. Meanwhile, the neighbors of non-leaders probably are non-leaders and in the same article team. So non-leaders have high LCCs, and collaborated non-leaders have similar degrees on average, which is a reason for positive PCCs of k and $N(k)$ in small k regions. In the above analysis, the sizes of article teams are approximated by their expected value. However, the existence of large article teams can increase the degree correlation coefficients. For example, the PCCs of k and $N(k)$ in the large k -regions are -0.025 and -0.045 for PNAS and Sub-PNAS respectively (Fig 8a). In addition, some non-leaders could leave their teams, so are unlikely to collaborate with new coming members. For example, many

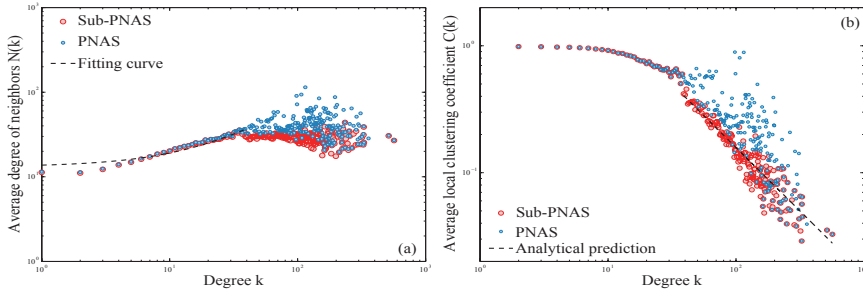


Fig. 8 The influence of large article teams on local clustering coefficients and average degree of node neighbors. The panels show the average local clustering coefficients and average degree of neighbors for nodes with degree k in Sub-PNAS and PNAS respectively.

students leave their research teams after graduations, so the students studied in different periods of time are unlikely to collaborate. The leaving also leads to the low LCC of leaders.

The description in above analysis is imitated by our model. The good model-data fit confirms the reasonability of the analysis. Especially, the phenomenon of research-team member leaving is imitated by shrinking the influential zones, which make some existing non-leaders no longer be the candidates of the new members' collaborators. Only those non-leaders, who are very close to the leaders in spacial distances, could write articles persistently. Above analysis is also partly confirmed by the decreasing trend appearing in the average proportion of the largest cliques in the components with size s (expect the giant, Fig 3b).

The theoretical analysis and calculation in Appendix show the tails of $C(k)$ of the modeled networks are proportional to $1/k$, which are similar to those of the empirical networks (Fig 6). This law is clear in DBLP-Math, but not so clear in PNAS (Fig 6). The reason is that PNAS has few large article teams, but the theoretical analysis is based on the mean size of article teams, and ignores large article teams (which occur at low-rates). This explanation is confirmed by the clear law in Sub-PNAS, which removes the large article teams (Fig 8b).

The model overcomes two fitting defects of our previous model in Ref [24], namely the $N(k)$ and $C(k)$ of modeled networks are more similar to those of the empirical data. For example, the increasing parts of $N(k)$ here are longer than those of our previous result with the same parameter μ (Fig 5 in Ref [24], Fig 6), a reason of which is described as follows. Suppose node i has an influence zone covers node j . The expected degrees of nodes i and j satisfy $k_i \approx \alpha(\theta_i)\delta t_i^{-\beta}T^\beta/\beta$ and $k_j \leq \mu \log(T/\max(m(\theta_i, t_i), t_j)) + \mu$ respectively. Hence the expected degree of i 's neighbors is larger than that of our previous model. This also makes the degree associativity of modeled networks do not require a large μ as our previous model does. A small μ makes the $P(k)$ (with a small hook head) and $C(k)$ (with a smooth transition) of Modeled network

2 are all similar to those of DBLP-Math (Figs 4b, 6b), and better than those of our previous result (Fig 4 in Ref [24]).

6 Conclusion

A growing geometric graph is proposed to model coauthorship networks with particular concern on the transition phenomena emerging in special features of those networks. The model overcomes some shortcomings of our previous model, and provides better predictions of some statistical features of the empirical data, e.g. the scaling relation between local clustering coefficient/average degree of neighbors and degree. The model potentially paves a geometric way to understand some aspects of collaboration modes. For example, it explains the emergence of generalized Poisson and power-law in degree distributions by the different collaboration modes of leaders and other team members of research teams.

Some shortcomings of the model are indicative of the need for further research: The increment of new nodes should not be fixed; New academic leaders could gain more collaborators than old ones; More reasonable expressions are needed for the academic communications between research teams. We are interested in the transition phenomena in citation networks, which are observed and analyzed by G.J. Peterson et al [32]. Is there any relation between the transition phenomena in citation networks and those in coauthorship networks?

References

1. Glänzel W, Schubert A (2004) Analysing scientific networks through co-authorship. Handbook of quantitative science and technology research, 257-276.
2. Mali F, Kronegger L, Doreian P, Ferligoj A, Dynamic scientific coauthorship networks (2012) In: Scharnhorst A, Börner K, Besselaar PVD editors. Models of science dynamics. Springer. pp. 195-232.
3. Glänzel W (2014) Analysis of co-authorship patterns at the individual level. *Transinformacao* 26: 229-238.
4. Sarigöl E, Pfitzner R, Scholtes I, Garas A, Schweitzer F (2014) Predicting scientific success based on coauthorship networks. *EPJ Data Science* 3(1): 1-16.
5. Bertsimas D, Brynjolfsson E, Reichman S, Silberholz JM (2014) Moneyball for academics: Network analysis for predicting research impact. Available at SSRN 2374581.
6. Newman M (2001) The structure of scientific collaboration networks. *Proc Natl Acad Sci USA* 98: 404-409.
7. Newman M (2001) Scientific collaboration networks. I. network construction and fundamental results. *Phys Rev E* 64: 016131.
8. Newman M (2001) Scientific collaboration networks. II. shortest paths, weighted networks, and centrality. *Phys Rev E* 64: 016132.
9. Newman M (2004) Coauthorship networks and patterns of scientific collaboration. *Proc Natl Acad Sci USA* 101: 5200-5205.
10. Barabási AL, Jeong H, Néda Z, Ravasz E, Schubert A, Vicsek T. (2002) Evolution of the social network of scientific collaborations. *Physica A* 311: 590-614.
11. Börner K, Maru JT, Goldstone RL (2004) The simultaneous evolution of author and paper networks. *Proc Natl Acad Sci USA* 101(suppl 1), 5266-5273.
12. Moody J (2004) The structure of a social science collaboration network: disciplinary cohesion from 1963 to 1999. *Am Sociol Rev* 69(2): 213-238.

13. Perc C (2010) Growth and structure of Slovenia's scientific collaboration network. *J Informetr* 4: 475-482.
14. Wagner CS, Leydesdorff L (2005) Network structure, self-organization, and the growth of international collaboration in science. *Res Policy* 34(10): 1608-1618.
15. Tomassini M, Luthi L (2007) Empirical analysis of the evolution of a scientific collaboration network. *Physica A* 285: 750-764.
16. Zhou T, Wang BH, Jin YD, He DR, Zhang PP, He Y, et al. (2007) Modeling collaboration networks based on nonlinear preferential attachment. *Int J Mod Phys C* 18: 297-314.
17. Milojević S (2014) Principles of scientific research team formation and evolution. *Proc Natl Acad Sci USA* 111: 3984-3989.
18. Catanzaro M, Caldarelli G, Pietronero L (2004) Assortative model for social networks. *Phys Rev E* 70: 037101.
19. Penrose M, *Random geometric graphs*, Oxford studies in probability, 2003.
20. Krioukov D, Kitsak M, Sinkovits RS, Rideout D, Meyer D, Boguñá M (2012) Network cosmology. *Sci Rep* 2: 793.
21. Xie Z, Ouyang ZZ, Zhang PY, Yi DY, Kong DX (2015) Modeling the citation network by network cosmology. *Plos One* 10(3): e0120687.
22. Xie Z, Ouyang ZZ, Liu Q, Li JP (2016) A geometric graph model for citation networks of exponentially growing scientific papers. *Physica A* 456: 167-175.
23. Xie Z, Rogers T (2016) Scale-invariant geometric random graphs. *Phys Rev E* 93: 032310.
24. Xie Z, Ouyang ZZ, Li JP (2016) A geometric graph model for coauthorship networks. *J Informetr* 10: 299-311.
25. Newman M (2002) Assortative mixing in networks. *Phys Rev Lett* 89: 208701.
26. Hoekman J, Frenken K, Tijssen RJW (2010) Research collaboration at a distance: Changing spatial patterns of scientific collaboration within Europe. *Res Policy* 39: 662-673.
27. Glänzel W (2011) National characteristics in international scientific co-authorship relations. *Scientometrics* 51: 69-115.
28. Xie Z, Duan XJ, Ouyang ZZ, Zhang PY (2015) Quantitative analysis of the interdisciplinarity of applied mathematics. *Plos One* 10(9): e0137424.
29. Blondel VD, Guillaume JL, Lambiotte R, Lefebvre E (2008) Fast unfolding of communities in large networks. *J Stat Mech* 10: P10008.
30. Consul PC, Jain GC (1973) A generalization of the Poisson distribution. *Technometrics* 15(4): 791-799.
31. Pastor-Satorras R, Vázquez A, Vespignani A (2001) Dynamical and correlation properties of the Internet. *Phys Rev Lett* 87(25): 258701.
32. Peterson GJ, Steve Pressé S, Dill KA (2010) Nonuniversal power law scaling in the probability distribution of scientific citations. *Proc Natl Acad Sci USA* 107: 16023-16027.

7 Appendix

7.1 The underlying formulae of degree distributions

Firstly, we analyze the degree distribution of the network, the edges of which are only generated by Rule (a) in Step 2. The overlapping probability of zones is small, because $\alpha(\cdot)$ is small (due to the limitation of the maximum degree). Hence the overlapping of zones is ignored in the following analysis. We choose a proper q to make the sizes of most hyperedges be drawn from the Poisson part f_1 with mean $\mu + 1$. We initially consider the effect of those hyperedges on the degree distribution, and next consider that of the hyperedges, the sizes of which are drawn from the power-law part f_2 .

Case 1: the degrees of the nodes having zones. Suppose node i has a zone. Let $S(\theta)$ be the smallest s satisfying $n(\theta, s, T) < \mu$. The expected degree

of node i contributed by Rule (a) in Step 2 is $k_a(\theta_i, t_i) \approx n(\theta_i, t_i, T)$ and the approximation holds for $t_i \ll T$. If $S(\theta)$ is large enough (which can be achieved by choosing proper parameters) we have a small $|\partial k_a(\theta_i, s)/\partial s|$ for $s > S(\theta)$, and so we take $k_a(\theta_i, s)$ to be independent of s and write $k_a(\theta_i)$ instead of $k_a(\theta_i, t_i)$.

Case 2: the degrees of the nodes having no zone. Assume node i is covered by a zone of node j . If $S(\theta_j) \leq t_j \leq T$, the expected degree of node i contributed by Rule (a) in Step 2, namely by being covered by the zone of j , is $k_a(t_i, \theta_j, t_j) \approx n(\theta_j, t_j, T) \approx k_a(\theta_j) \approx k_a(\theta_i)$, where the third approximation is due to the small distance $d(\theta_i, \theta_j)$ and the piecewise constant property of $\alpha(\cdot)$. Now we suppose $t_j < S(\theta_j)$. Let $m(\theta_j, t_j)$ be the smallest s satisfying $n(\theta_j, t_j, s) > \mu$ and $k_a(t_i, \theta_j, t_j, s)$ be the expected degree of node i at time s . Since the nodes fall randomly and uniformly, the probability of any existing node in the current influential zone of a leader connecting to a new node is equal. Hence the rate at which node i acquires edges from the nodes coming at time s satisfies

$$\begin{aligned} \partial k_a(t_i, \theta_j, t_j, s)/\partial s &\leq (\mu - 1) \times \alpha(\theta_j) \delta t_j^{-\beta} s^{\beta-1} \times n(\theta_j, t_j, s-1)^{-1} \\ &\approx \beta(\mu - 1)/s. \end{aligned} \quad (2)$$

Therefore $k_a(t_i, \theta_j, t_j) \leq \beta(\mu - 1) \log(T/\max(m(\theta_j, t_j), t_i)) + \mu$. If t_i is large enough, $k_a(t_i, \theta_j, t_j) \approx \mu$. In addition, $k_a(t_i, \theta_j, t_j) < \beta(\mu - 1) \log(T) + \mu$ so can not effect the tail of the degree distribution.

The degrees of nodes will not be exactly equal to their expected values because the nodes are distributed according to a Poisson point process, and so need to be averaged with the Poisson distribution. In addition, the nodes of the hyperedges with large sizes drawn from f_2 would not have small degrees. Hence the degree distribution of small degree nodes is

$$\begin{aligned} P_S(k) &= \frac{1}{2\pi} \int_0^{2\pi} \left(\frac{\epsilon(\theta) k_a(\theta)^k e^{-k_a(\theta)}}{k!} + \frac{1 - \epsilon(\theta)}{S(\theta) - 1} \sum_{t=1}^{S(\theta)-1} \left(\frac{1}{T - m(\theta, t) + 1} \right. \right. \\ &\quad \left. \left. \times \sum_{s=m(\theta, t)}^T \frac{k_a(s, \theta, t)^k e^{-k_a(s, \theta, t)}}{k!} \right) \right) d\theta, \end{aligned} \quad (3)$$

where $\epsilon(\theta)$ is the proportion of the nodes covered by the zones of the nodes born on or after time $S(\theta)$. Eq (3) is a mixture of some Poisson distributions with different expected values, namely the expected degree in small k regain is not a constant. Meanwhile, the probability of adding a new neighbor for a given node is affected by the spacial locations of previous leaders. Therefore, it is also reasonable to consider that the predominant modeled collaborations are govern by certain generalization of Poisson processes.

The calculation for the degree distribution in large k region is the same as that in Ref [24], and so is briefly listed as follows:

$$P_L(k) = \frac{1}{2\pi k!} \int_0^{2\pi} \left(\frac{1}{S(\theta)} \int_1^{S(\theta)+1} k_a(\theta, t, T)^k e^{-k_a(\theta, t, T)} dt \right) d\theta \propto \frac{1}{k^{1+\frac{1}{\beta}}}, \quad (4)$$

where $k \gg 0$ is needed in the calculation.

The hyperedges with large sizes drawn from f_2 can affect the tail of degree distribution. Ignoring the overlapping of those hyperedges (which is due to the small probability of their occurrences) and the proportion of the nodes having zones and belonging to those hyperedges (which is small when compared with that of the nodes having no zone) we obtain that the degree distribution's tail of the network generated by Rule (a) in Step 2 is approximately a mixture power-law distribution $qP_L(k) + (1-q)(k+1)f_2(k+1)/\sum_s s f_2(s)$.

Finally, we analyze the degrees contributed by Rule (b). Let $k_b(\theta_i, t_i, s)$ be the degree of node i contributed by this rule at time $s \geq t_i$. The number of nodes with nonzero degree at time s is $N(s) = \zeta \int_0^{2\pi} (\sum_{t=1}^s \alpha(\theta) \delta t^{-\beta} s^\beta / \beta) d\theta \approx s \delta \zeta \int_0^{2\pi} \alpha(\theta) d\theta / (\beta(1-\beta))$, where $\zeta = N_2/(2\pi)$. So the probability that a node is chosen by Rule (b) of Step 2 at time s is $(\nu+1)N_3/N(s)$, where $\nu+1$ is the expected value of f in Rule (b) in Step 2. Hence, the rate at which node i at time s acquires edges generated by Rule (b) is $\partial k_b(t_i, s)/\partial s = \nu(\nu+1)N_3/N(s)$, which gives $k_b(t_i, T) \approx \beta(1-\beta)\nu(\nu+1) \log(T/t_i)N_3/(\delta \zeta \int_0^{2\pi} \alpha(\theta) d\theta)$. Hence, choosing proper parameters, the degrees contributed by Rule (b) can be ignored, when compared with that contributed by Rule (a) in Step 2.

In simulations, the condition $k \gg 0$ required in Eq (4) can not be fully satisfied due to the restriction of the maximum degree, which is a reason for the difference between the theoretical value and the practical value of the power exponent. However, the degree distributions of the modeled networks fit the above analysis at certain levels, and are similar to those of the empirical networks respectively (Fig 4).

7.2 The underlying formulae of the correlation of local clustering coefficients and degrees

Suppose node i has a zone and t_i is small enough. So the number of neighbors of node i generated by Rule (b) in Step 2 can be ignored compared with that generated by Rule (a). Hence the expected degree k of i is approximately equal to $k_a(\theta_i, t_i, T)$. Suppose nodes j, l belong to the zone and $t_j < t_l$. Since t_i is small, k is large, so $T - m(\theta_i, t_i) \approx T - T(\mu/k)^{1/\beta} \approx T$, where $m(\theta_i, t_i)$ is the smallest s satisfying $n(\theta_i, t_i, s) > \mu$. So we can only consider the case $t_j > m(\theta_i, t_i)$. Since the nodes are dropped randomly and uniformly, the probability of an edge between j and l is $\omega T^\beta / (k(t_l - 1)^\beta)$ the reciprocal of the number of nodes (born before t_l) of the zone multiplied by ω , the expected hyperedge size less than two, where the boundary effects of zones are ignored. Averaging over possible values of t_j and t_l , the LCC of node i is

$$\begin{aligned} C(k) &= \frac{1}{T - m(\theta_i, t_i)} \int_{m(\theta_i, t_i)}^T \left(\frac{1}{T - t_j - 1} \int_{t_j+1}^T \frac{\omega T^\beta}{k(t_l - 1)^\beta} dt_l \right) dt_j \\ &\approx \frac{\omega T^{\beta-1}}{k(1-\beta)} \left(\int_{m(\theta_i, t_i)}^T \frac{(T-1)^{1-\beta} - s^{1-\beta}}{T-s-1} ds \right), \end{aligned} \quad (5)$$

where the approximation holds for $T \gg m(\theta_i, t_i)$. Denote the coefficient of $1/k$ by $I(k)$, substitute $m(\theta_i, t_i) \approx T(\mu/k)^{1/\beta}$ into it, and differentiate it to obtain

$$\frac{dI(k)}{dk} = \frac{\omega T^{\beta-1}}{1-\beta} \times \frac{(T-1)^{1-\beta} - T^{1-\beta} \left(\frac{\mu}{k}\right)^{\frac{1-\beta}{\beta}}}{T - T \left(\frac{\mu}{k}\right)^{\frac{1}{\beta}} - 1} \times \frac{T}{\beta} \frac{\mu^{\frac{1}{\beta}}}{k^{\frac{1}{\beta}+1}} \approx \frac{\omega \mu^{\frac{1}{\beta}}}{\beta(1-\beta)k^{\frac{1}{\beta}+1}}, \quad (6)$$

which is approximately equal to 0 if $k \gg \mu$. Hence $I(k)$ is free of k and $C(k) \propto 1/k$ if k is large enough. The modeled networks roughly follow the above analyses (Blue diamonds in Fig 6), in which the outliers are partly caused by the boundary effects of zones that can not be ignored under the occurrence of some large size hyperedges drawn from $f_2(x)$.